Journal of Neurochemistry

JOURNAL OF NEUROCHEMISTRY | 2011 | 118 | 749–759 doi: 10.1111/j.1471-4159.2011.07352.x

ORIGINAL ARTICLE

In vivo electrochemical evidence for simultaneous 5-HT and histamine release in the rat substantia nigra pars reticulata following medial forebrain bundle stimulation

Parastoo Hashemi,* Elyse C. Dankoski,† Kevin M. Wood,* Rebecca Ellen Ambrose* and Robert Mark Wightman*,†

*Department of Chemistry, University of North Carolina at Chapel Hill, Chapel Hill, North Carolina, USA

†Curriculum in Neurobiology, University of North Carolina at Chapel Hill, Chapel Hill, North Carolina, USA

Abstract

Exploring the mechanisms of serotonin [5-hydroxytryptamine (5-HT)] in the brain requires an *in vivo* method that combines fast temporal resolution with chemical selectivity. Fast-scan cyclic voltammetry is a technique with sufficient temporal and chemical resolution for probing dynamic 5-HT neurotransmission events; however, traditionally it has not been possible to probe *in vivo* 5-HT mechanisms. Recently, we optimized fast-scan cyclic voltammetry for measuring 5-HT release and uptake *in vivo* in the substantia nigra pars reticulata (SNR) with electrical stimulation of the dorsal raphe nucleus (DRN) in the rat brain. Here, we address technical challenges associated with rat DRN surgery by electrically stimulating 5-HT projections in the medial forebrain bundle (MFB), a more accessible anatomical location. MFB stimulation elicits 5-HT in the SNR; furthermore, we find simultaneous release of an additional species. We use electrochemical and pharmacological methods and describe physiological, anatomical and independent chemical analyses to identify this species as histamine. We also show pharmacologically that increasing the lifetime of extracellular histamine significantly decreases 5-HT release, most likely because of increased activation of histamine H-3 receptors that inhibit 5-HT release. Despite this, under physiological conditions, we find by kinetic comparisons of DRN and MFB stimulations that the simultaneous release of histamine does not interfere with the quantitative 5-HT concentration profile. We therefore present a novel and robust electrical stimulation of the MFB that is technically less challenging than DRN stimulation to study 5-HT and histamine release in the SNR.

Keywords: fast-scan cyclic voltammetry, histamine *N*-methyltransferase, medial forebrain bundle, serotonin, SKF 91488, substantia nigra pars reticulata.

J. Neurochem. (2011) **118**, 749–759.

5-hydroxytryptamine (5-HT) is an important neuromodulator and dysfunctions of the 5-HT system are particularly well-documented in neurological disorders such as anxiety and depression (Petty *et al.* 1996). *In vivo* neurochemical measurements of 5-HT are necessary for furthering our understanding of the mechanisms that govern these disorders, and will improve their diagnosis and treatment. Microdialysis studies have correlated *in vivo* basal level 5-HT changes to behavioral and pharmacological manipulations (Rueter *et al.* 1997; Barnes and Sharp 1999). Basal 5-HT levels are determined by numerous individual neurotransmission events that are averaged in one microdialysis reading (Robinson and Wightman 2007) and to fully understand the mechanisms that underlie these slow changes requires quantitative, subsecond endogenous 5-HT detection. This has

Received March 9, 2011; revised manuscript received June 8, 2011; accepted June 10, 2011.

Address correspondence and reprint requests to R. Mark Wightman, Department of Chemistry, University of North Carolina at Chapel Hill, Chapel Hill, NC 27599, USA. E-mail: rmw@unc.edu

Abbreviations used: 5-HT, 5-hydroxytryptamine; DRN, dorsal raphe nucleus; FSCV, fast-scan cyclic voltammetry; MFB, medial forebrain bundle; SNR, substantia nigra pars reticulata; TM, tuberomammillary nucleus.

traditionally been accomplished with fast-scan cyclic voltammetry (FSCV) in tissue slice preparations (O'Connor and Kruk 1991; Rice *et al.* 1994; Bunin and Wightman 1998; John *et al.* 2006). These studies have provided a solid understanding of 5-HT release and uptake kinetics (Bunin *et al.* 1998), 5-HT receptor pharmacology (Davidson and Stamford 1996; Threlfell *et al.* 2010), and 5-HT metabolism by monoamine oxidase (John and Jones 2007). Recently, FSCV has been used to perform similar characterizations in *D. melanogaster* (Borue *et al.* 2009, 2010). While these types of studies are essential to describe basic 5-HT mechanisms, *in vivo* measurements in a mammalian brain are necessary to understand how 5-HT dynamics are modulated in the complex entity of the intact nervous system. Recently we described a FSCV technique in which carbon-fiber microelectrodes were coated with Nafion to monitor 5-HT *in vivo* (Hashemi *et al.* 2009). The Nafion modification reduces electrode fouling while increasing its sensitivity to 5-HT. This is the first technique capable of monitoring endogenous, *in vivo* 5-HT release and uptake on a subsecond time scale. In this previous work, we established a physiological model where we evoked 5-HT release with a bipolar stimulating electrode in the dorsal raphe nucleus (DRN), the location of 5-HT cell bodies, and recorded terminal 5-HT release and uptake in the substantia nigra pars reticulata (SNR) (Hashemi *et al.* 2009).

In this paper, we explore an alternative method of evoking 5-HT release in the SNR. Using the well-documented efferent circuitry of the DRN (Azmitia and Segal 1978; Moore *et al.* 1978; Parent *et al.* 1981; Imai *et al.* 1986), we exploit a branched 5-HT projection to both the SNR and the striatum (van der Kooy and Hattori 1980; Imai *et al.* 1986) that is located in the medial forebrain bundle (MFB). We previously showed that electrical stimulation of the MFB released an unidentified substance in the red nucleus of the rat that we suspected was 5-HT (Kita *et al.* 2009). This suggested that MFB stimulation could evoke 5-HT release in targets posterior to the stimulating electrode. Here, we confirm this expectation by demonstrating that branched 5-HT fibers can be retrogradely activated, allowing the experimenter to avoid targeting the DRN, an anatomically challenging surgical technique. However, we find that MFB stimulation elicits release of an additional species in the SNR. With electrochemical and pharmacological data, in addition to literature documenting histamine's physiological, anatomical and independent chemical verification in the SNR (Brown *et al.* 2001), we identify this substrate as histamine. Threllfel *et al.* have previously shown that pharmacological activation of H-3 receptors inhibits 5-HT release (Threlfell *et al.* 2004). In accord with this, we find significant decreases in 5-HT release upon administration of SKF 91488, an agent that prolongs histamine lifetime in the synapse. With no drug present, we compare the 5-HT concentration release and uptake profiles between DRN and MFB stimulations and find that histamine release does not interfere with the quantification of the 5-HT signal. We thereby present a novel and robust method for studying 5-HT and histamine neurotransmission in the SNR.

Materials and methods

Animals

Male Sprague–Dawley rats, 8–12 weeks old, weighing 250–350 g, were purchased from Charles River Labs (Raleigh, NC, USA). Rats were housed under 12 h/12 h light cycles with controlled temperature and humidity. Food and water were available *ad libitum*. All animal care was in accordance with the Guide for the Care and Use of Laboratory Animals and was approved by the Institutional Animal Care and Use Committees of the University of North Carolina.

Surgery

Rats were anesthetized with urethane (1.5 g/kg rat weight) and positioned into a stereotaxic frame (David Kopf Instruments, Tujunga, CA, USA). Holes were drilled in the skull according to stereotaxic coordinates referenced from bregma and taken from Paxinos and Watson's Rat Brain Atlas (Paxinos and Watson 2007). Nafion-modified carbon-fiber microelectrodes were implanted in the SNR (stereotaxic coordinates AP −4.8 to −5.2; ML +2.0; DV −8.5). A bipolar stainless steel stimulating electrode, insulated to the tip (0.2 mm diameter, Plastics One, Roanoke, VA, USA) was implanted into the MFB (AP −2.5 to −2.8; ML 1.7; DV −8.0) or DRN as described previously (Hashemi *et al.* 2009). An Ag/AgCl wire serving as a reference electrode was implanted into the contralateral hemisphere. Computer-generated biphasic pulse trains were applied through constant current stimulators (NL 800A, Neurolog, Medical Systems Corp., Great Neck, NY, USA), 2 ms in width and 350 μA each phase (unless otherwise noted), at 60 Hz for 2 s to evoke 5-HT release.

Voltammetric procedures

Cylindrical carbon-fiber microelectrodes were constructed by aspiration of a single 2.5-μm radius carbon fiber (T-650, Thornel, Amoco Co, Greenville, SC, USA) into a glass capillary of 0.6 mm external diameter and 0.4 mm internal diameter (A-M Systems, Inc., Sequim, WA, USA). A micropipette puller (Narishige, Tokyo, Japan) was used to taper the glass and form a carbon-glass seal. The exposed carbon fiber was cut to approximately 100 μm in length and was soaked for 30 min in isopropyl alcohol to clean the surface. The procedure for electrodeposition of Nafion was described previously (Hashemi *et al.* 2009). Dopamine and 5-HT specific electrochemical detection waveforms were used as described elsewhere (Jackson *et al.* 1995; Heien *et al.* 2003). A customized version of TH-1 software (ESA, Chelmsford, MA, USA) written in LABVIEW (National Instruments, Austin, TX, USA) was used for waveform generation and data acquisition. A custom-built UEI potentiostat (University of North Carolina at Chapel Hill, Department of Chemistry Electronics Facility) was employed. All potentials are reported versus an Ag/AgCl reference electrode. Signal processing [background subtraction, signal averaging, and digital filtering (4-pole Bessel Filter, 5 kHz)] was also done in TH-1

software. Voltammetric data are visualized as color plots that show multiple background-subtracted cyclic voltammograms that were consecutively collected. The abscissa is time and the current is encoded as false color (Michael *et al.* 1998). For most of the work in this paper, the ordinate is the voltage axis that peaks at 1.0 V, scans back to −0.1 V and returns to 0.2 V, the rest potential. The sensitivity with this waveform on Nafion modified microelectrodes to 5-HT is 49.5 nA/μM and 0.4 nA/μM to histamine.

Histology

To verify the spatial placement of the electrodes *in vivo*, the carbon-fiber microelectrode that acquired data was used to create a small, specific lesion in the recording site by applying constant voltage (20 V for 10 s) (Park *et al.* 2009). Following the experiment, rats were killed and perfused with 10% formalin solution. Brains were then removed from the skull and stored in 10% formalin. After at least 3 days, the brains were flash-frozen, sectioned into 40 μm slices in a cryostat, mounted on glass slides, and stained with 0.2% thionine. The brains were visualized and photographed with an optical microscope.

Drugs and reagents

Serotonin hydrochloride, histamine dihydrochloride and thioperamide maleate were obtained from Sigma-Aldrich (St. Louis, MO, USA) at reagent quality and used without purification. SKF 91488 dihydrochloride was obtained from Tocris Bioscience (Ellisville, MO, USA) and was delivered at a high dose to ensure permeation across blood brain barrier and cause robust *in vivo* effects (50 mg/kg). Drugs were dissolved in saline and were injected intraperitoneally at a volume of 0.6 mL/kg.

Data analysis

Kinetic characterization of 5-HT release and uptake was adapted from techniques previously used to describe kinetics of release and uptake of the dopamine system (Garris and Wightman 1994). Release was described as $[5\text{-HT}]_p * f$, where $[5\text{-HT}]_p$ is the amount of 5-HT released per stimulation pulse, and f is the frequency of stimulation pulses. The rate of change during stimulation is:

$$\frac{d[5\text{-HT}]}{dt} = [(5\text{-HT})_p * f] - \left\{\frac{d[5\text{-HT}]}{dt}\right\}_{uptake} \quad (1)$$

in which the duration of the release term is determined by the number of pulses in the stimulation. Only the uptake term dominates after the stimulation terminates. The uptake rate of 5-HT from the extra-cellular space (v) following electrically stimulated release was assumed to follow the Michaelis–Menten equation:

$$v = \left\{\frac{d[5\text{-HT}]}{dt}\right\}_{uptake} = \frac{V_{max}}{\frac{K_m}{[5-HT]} + 1} \quad (2)$$

V_{max} is the maximal rate of uptake, and K_m is the Michaelis–Menten constant that describes the affinity of the 5-HT transporter for 5-HT. It was taken to be 170 nM, a value found in rat brain synaptosomes (Shaskan and Snyder 1970; Mosko *et al.* 1977).

In all simulations, analyte diffusion through a thin layer (300 nm) of Nafion was accounted for (Kristensen *et al.* 1987). The amount of 5-HT released per stimulation pulse $[(5\text{-HT})_p]$ and K_m and V_{max} were determined by fitting the model to the experimental data. In experiments involving transport inhibition, V_{max} was fixed to values determined in pre-drug models.

Student's *t*-tests were performed on paired data sets, $p < 0.05$ was taken as significant.

Flow injection analysis

For experiments characterizing histamine and 5-HT cyclic voltammetry *in vitro*, flow injection analysis was used (Kristensen *et al.* 1986). The carbon-fiber microelectrode was placed in the output of a six-port HPLC loop injector mounted on a two-position actuator (Rheodyne model 7010 valve and 5701 actuator), operated by a 12 V DC solenoid valve kit (Rheodyne, Rohnert Park, CA, USA). The apparatus enabled the introduction of a rectangular pulse of analyte to the microelectrode surface using a syringe infusion pump (Harvard Apparatus model 940, Hollison, MA, USA) at a flow rate of 2 mL/min.

For *in vivo* experiments, the recording electrode was used to make a lesion in the tissue at the end of all experiments to verify its placement histologically. The high voltage across the working electrode used to achieve this necessarily over-oxidizes the carbon surface altering its sensitivity. Therefore, post-calibrations would not be a reliable measure of the electrode response. Rather, pre-calibrations were used to obtain a calibration curve, as described previously (Hashemi *et al.* 2009).

Results

Comparison of 5-HT following DRN or MFB stimulation

Histology verified the location of the stimulating and carbon-fiber microelectrodes in coronal slices of brains used in *in vivo* experiments (Fig. 1). The stimulating electrode was in the MFB and the carbon-microelectrode was in the SNR as indicated by the small lesions.

We have previously shown that electrical stimulation of the DRN releases 5-HT in the SNR (Hashemi *et al.* 2009). In Fig. 2, we compare this type of electrically stimulated 5-HT release (Fig. 2a) to 5-HT release elicited via MFB stimulation (Fig. 2b). The horizontal dashed lines in Fig. 2(a-iii) are at the peak potential for 5-HT oxidation (0.65 V) (1) and oxidation of an additional substrate (0.85 V) (2). The currents at these potentials were converted to concentrations and are plotted directly above this [(i) 5-HT, (ii) additional substrate]. In Fig. 2(a-i), the current begins to rise at stimulus initiation and peaks within 0.5 s of the stimulation termination. In Fig. 2(a-ii), there is a small increase in current in response to the stimulation. The vertical dashed line in the color plot (Fig. 2a-iii) at the end of the stimulation and the current at this time were used to construct the cyclic voltammogram (inset). This cyclic voltammogram is identical to those obtained *in vitro* for 5-HT where the presence of the reverse wave is characteristic of 5-HT. Similar results were obtained with MFB stimulation (Fig. 2b). In Fig. 2(b-i), the 5-HT current profile closely matches the 5-HT current profile in Fig. 2(a-i), however, the current obtained upon

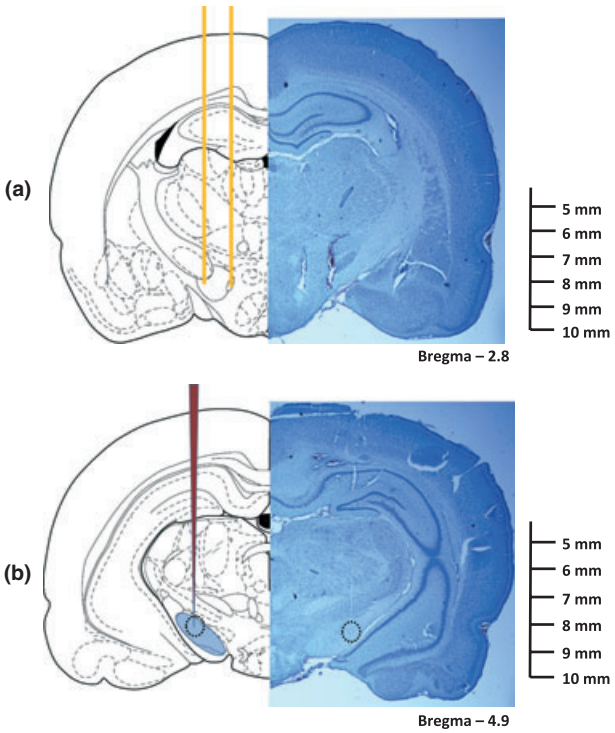

Fig. 1 Histology of stimulating and carbon-fiber electrode placements in the MFB and SNR. Left hemisphere is a diagram showing intended placement of (a) stimulation electrode in the MFB or (b) carbon fiber microelectrode in the SNR at coordinates described in the methods section. Right hemisphere shows actual placement in a representative brain.

stimulation in Fig. 2(b-ii) is threefold greater with MFB stimulation that with DRN stimulation. The cyclic voltammogram (inset α) is taken at the vertical dashed line at the end of the stimulation. An additional vertical dashed line (β) is taken 2 s after the stimulus termination; the current at this time was used to construct the cyclic voltammogram in inset β. Panel (c) shows the averaged maximal release amplitudes of (1) 5-HT and (2) the additional substrate as the stimulating electrode is lowered down the dorsal/ventral tract above the MFB (n = 6 ± SEM). For each line, the data are normalized to the maximal signal along the stimulation track. When two points are statistically different, the p-value is noted.

The concentration changes extracted from the current at 0.65 V exhibit a time-course in the SNR very similar to the DRN stimulation. DRN and MFB averaged maximal concentrations in the SNR are statistically identical: 12.7 ± 1.6 nM (n = 6 ± SEM) 5-HT with DRN stimulation (Hashemi *et al.* 2009) and 12.8 ± 1.0 nM (n = 6 ± SEM) with MFB (p = 0.29). Similarly, the time for 5-HT to be cleared to one half of its maximal value ($t_{1/2}$) is 1.7 ± 0.3 s with DRN stimulation (n = 6 ± SEM) and 1.8 ± 0.2 s with MFB stimulation (n = 6 ± SEM) (p = 0.45).

Examination of the color plot reveals additional features around the time of the stimulation. An oxidation process at 0.85 V on the reverse scan accompanied by a reduction process at 0.1 V are simultaneous with the 5-HT signal. Because these processes disappear rapidly after the stimulation, a cyclic voltammogram collected at 2 s after the stimulation (inset β) has the characteristic 5-HT cyclic voltammogram. However, when it is recorded at the end of the stimulation (inset α), it has additional features. Because 5-HT is oxidized at a potential that is reached before the additional species, the presence of the second species does not distort the time-course of 5-HT detection.

Characterization of histamine cyclic voltammetry

The additional oxidation and reduction occur on the backwards oxidation scan and forwards reduction scan. This indicates a kinetically limited reaction that is dependent on the initial sweep that regenerates the electrode's carbon surface (Takmakov *et al.* 2010). The SNR is populated with histaminergic terminals (Panula *et al.* 1989) and histamine displays this type of kinetically limited electrochemistry as demonstrated by following the direction of the potential sweep with the arrows in Fig. 3. This figure compares *in vitro* responses at a carbon-fiber microelectrode, using the 5-HT waveform (see above) of (a) 5-HT (500 nM), (b) histamine (20 μM), (c) 5-HT + histamine (500 nM + 20 μM, respectively) to (d) the *in vivo* response in the SNR during MFB stimulation. Panel (i) shows the color plots and panel (ii) shows the cyclic voltammograms taken at the white dashed vertical lines. The microelectrode's response to histamine (20 μM) injected alone is 7.9 ± 0.9 nA (n = 4 ± SEM) and to histamine (20 μM) injected with 5-HT is 7.5 ± 0.7 nA (n = 4 ± SEM) (p = 0.6). The features of the *in vivo* response (d) are clearly electrochemically reproduced via a 5-HT + histamine mixture (c).

Figure 4 shows how the histamine signal changes with the applied waveform. Figure 4(a) shows a log-log trace of the current response (n = 5 ± SEM) *in vitro* to flow injections of histamine (20 μM) as a function of increasing the scan rate of the detection waveform. It can be seen that the histamine response is proportional to the scan rate: the slope of the log-log plot is 0.56 indicating diffusion-controlled electrochemistry. In Fig. 4(b), the peak amplitude for histamine oxidation is shown as a function of increasing the positive limit of the applied voltage. Increasing the potential window of the detection waveform causes an increase in the histamine response from 6.6 ± 2.2 nA (n = 5 ± SEM) at 1.2 V to 13.4 ± 3.7 nA (n = 5 ± SEM) at 1.3 V (p = 0.01). This behavior has been seen previously for dopamine (Hafizi *et al.* 1990). At the same time, the peak on the reverse scan occurs at more positive potentials as the scan limit is increased, shown by the inset cyclic voltammograms.

Responses to inhibition of histamine *N*-methyltransferase

Unlike most biogenic amine neurotransmitters, histamine is not thought to be inactivated by a specific transporter (Brown

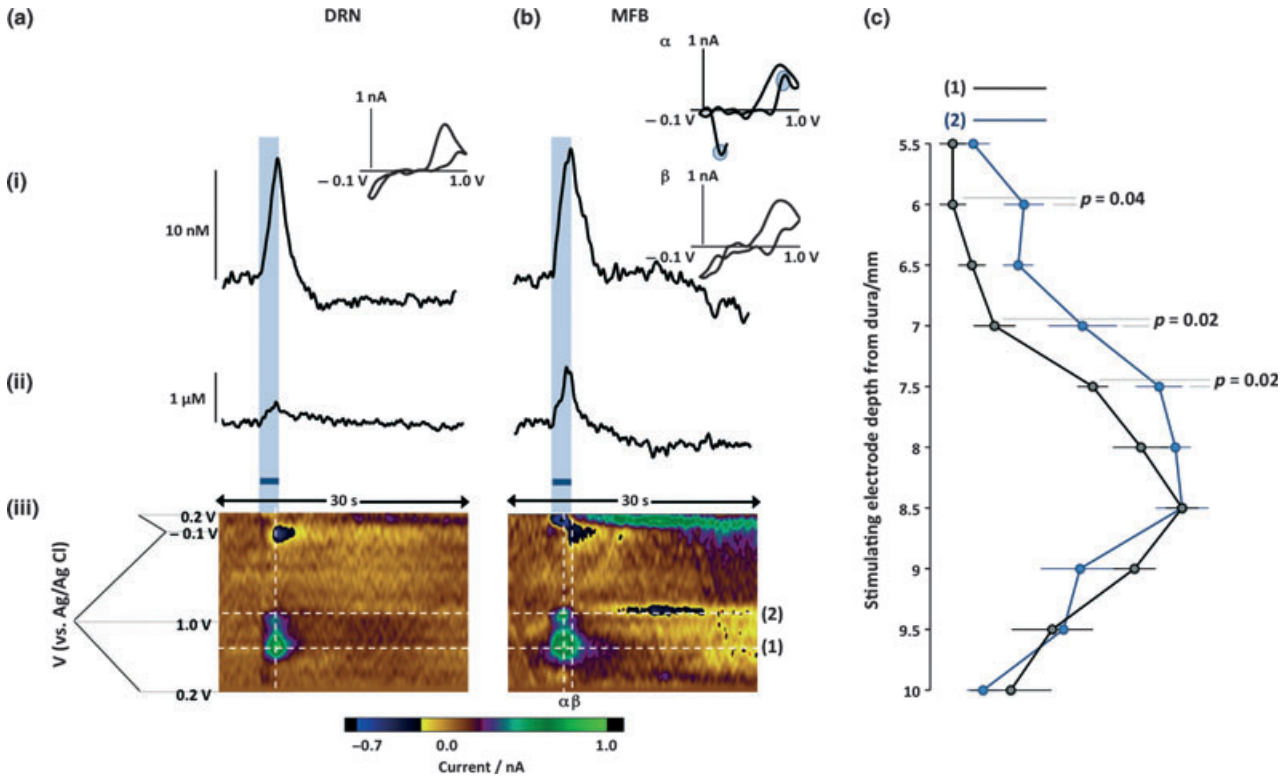

Fig. 2 5-HT color plot, CV and time profile of response in SNR with DRN and MFB stimulation. (a) and (b) – comparison of signals obtained in SNR obtained following DRN and MFB electrical stimulation, respectively. Concentrations vs. time taken at the horizontal white dashed lines are shown above the color plots in panels (i) and (ii), and representative cyclic voltammograms (vs. Ag/AgCl) taken at the vertical white dashed lines are inset. (iii) Color plots show all of the background corrected cyclic voltammetric data. Bipolar stimulation onset at 5 s is 350 µA, 60 Hz and 120 pulses, represented by blue bar. (c) shows averaged, normalized maximal release amplitude of 5-HT (1) and the additional substrate (2) at 0.5 mm dorsal/ventral intervals of the stimulating electrode (n = 6 ± SEM). Where the two values are statistically different, the p-value is added.

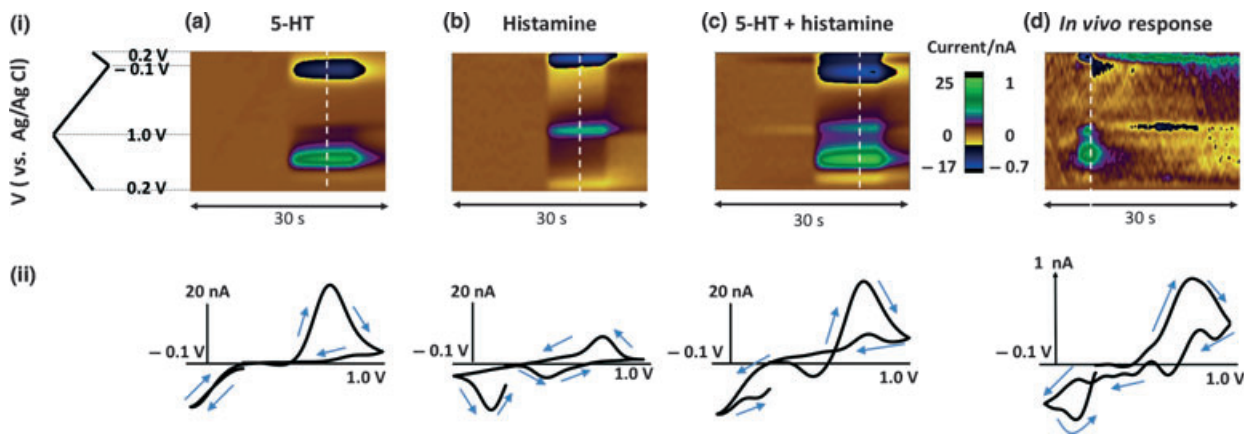

Fig. 3 Comparison of *in vivo* signal to a mixed *in vitro* 5-HT and histamine signal. *In vitro* injections of (a) 5-HT (500 nM), (b) histamine (20 µM), or (c) 5-HT (500 nM) + Histamine (20 µM), and (d) *in vivo* response shown in (i) color plot format and (ii) cyclic voltammograms. Current is represented in false color and is a dual scale (left for *in vitro* and right for *in vivo*). Representative cyclic voltammograms were taken at the white dashed lines; in (d), the cyclic voltammogram was taken at 0.5 s after stimulation duration, indicated by the white dashed line. This position best captures both substrates.

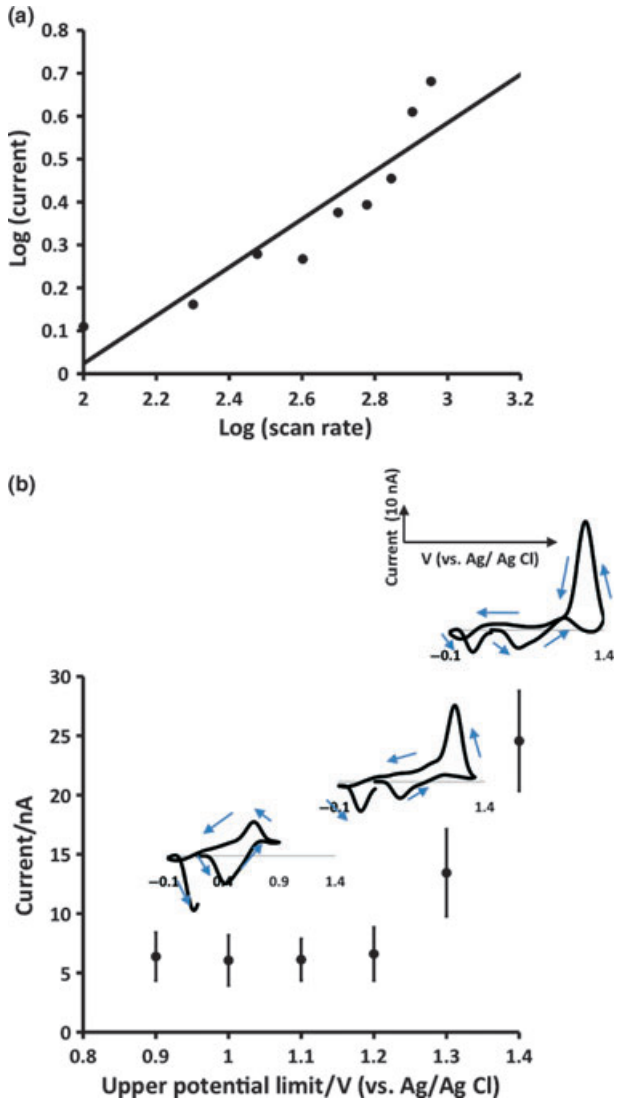

Fig. 4 Effect of varying scan rate and upper potential limit on histamine response *in vitro*. (a) Log-log current response to *in vitro* injections of histamine (20 μM) as the waveform scan rate is increased from 100 V/s to 2000 V/s with conventional 5-HT waveform (0.2–1.0 V) (n = 5 ± SEM), where the line of best fit is a linear regression. (b) Current response to *in vitro* injections of histamine (20 μM) as the upper potential window is increased from 0.9 V to 1.4 V (n = 5 ± SEM) vs. Ag/AgCl. Representative cyclic voltammograms are inset at 1.0, 1.3 and 1.4 V.

et al. 2001). Instead, it is primarily inactivated by methylation, a process that is catalyzed by histamine *N*-methyltransferase. To pharmacologically verify the species detected at more positive potentials as histamine, an inhibitor of histamine *N*-methyltransferase, SKF 91488 (50 mg/kg) was administered. SKF 91488 is a potent, non-competitive inhibitor of histamine *N*-methyltransferase that is inactive at histamine receptors (Beaven and Shaff 1979). Panel (i) of Fig. 5 displays the effects of this agent in one rat. Figure 5(a) shows the average color plot of five control stimulations, taken 10 min apart. Figure 5(b) shows the average color plot of five stimulations 1 h after drug administration, taken 10 min apart. Horizontal white dashed lines α and β were used to construct concentration vs. time plots of histamine (α) and 5-HT (β) which were then averaged for five animals and displayed in panel (ii) (n = 5 ± SEM). The control responses are shown in blue and the drug responses are shown in black. Electrically stimulated histamine release was 2.8 ± 1.3 μM (n = 5 ± SEM). After drug administration, the half-decay time ($t_{½}$) for histamine was significantly increased from 4.1 ± 0.9 s to 10.4 ± 2.1 s (p = 0.03) with no change in amplitude. The maximal evoked concentration of 5-HT decreased from 9.3 ± 1.0 nM to 4.6 ± 0.4 nM (p = 0.01) without a change in its $t_{½}$ value. Panel (iii) of Fig. 5 shows the effects of SKF 91488 on 5-HT release amplitude in control rats (a) (n = 5 ± SEM) and in rats pre-treated with thioperamide (10 mg/kg) (n = 6 ± SEM), a selective H-3 receptor antagonist (b). In rats pre-treated with thioperamide, 5-HT release is not significantly affected after SKF 91488 administration; the control response was 10.2 ± 1.3 nM and 10.4 ± 1.5 nM after SKF 91488 administration (p = 0.76).

Modeling 5-HT release and uptake

Figure 6 compares experimental and modeled 5-HT data between the two stimulations. The experimental data (blue dots) are superimposed on the model (black line). The model is a composite of linear release and uptake governed by Michaelis–Menten kinetics (Wightman *et al.* 1988). The concentration of 5-HT released per stimulation pulse, $[5\text{-HT}]_p$, and the maximal uptake velocity, V_{max}, were adjusted for the best fit while the value of the K_m for uptake was fixed at 170 nM. During DRN stimulation, the model yields $[5\text{-HT}]_p$ of 1.5 nM and a V_{max} of 0.63 μM/s, and during MFB stimulation, the model yields $[5\text{-HT}]_p$ of 1.1 nM, with a V_{max} of 0.67 μM/s.

Discussion

Electrical MFB stimulation evokes 5-HT release in the SNR

The efferent circuitry of the DRN to the SNR is well-documented (Dray *et al.* 1976; Fibiger and Miller 1977; Wirtshafter *et al.* 1987; Corvaja *et al.* 1993), as are its projections to the striatum (Miller *et al.* 1975; Steinbusch *et al.* 1980, 1981). Some studies, including a retrograde labeling study by Van der Kooy *et al.*, show that the same 5-HT projection branches to both the SNR and the striatum (van der Kooy and Hattori 1980; Imai *et al.* 1986). Striatal bound 5-HT fibers travel within the MFB (Miller *et al.* 1975). If axonal stimulation in the MFB could be used in place of DRN stimulation, certain experimental challenges associated with DRN stimulation can be avoided. These challenges arise primarily from the small size, inaccessible

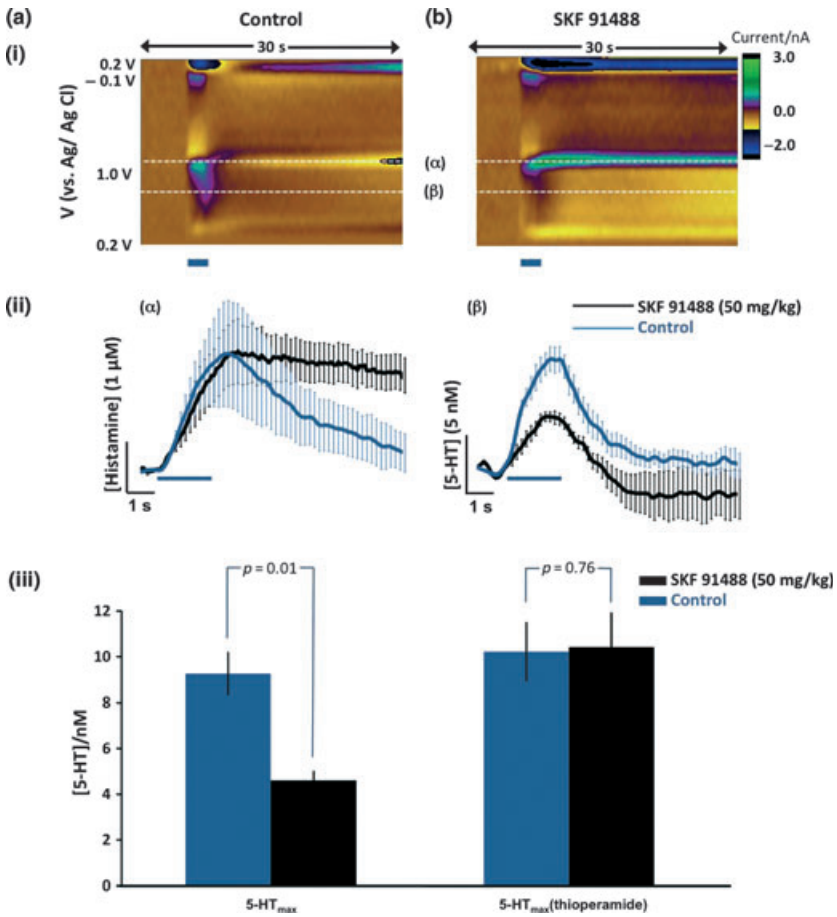

Fig. 5 Pharmacological characterization of histamine with SKF 91488. (i) Color plots showing electrically stimulated response in the SNR in (a) control and (b) 1 h after intra-peritoneal SKF 91488 (50 mg/kg) administration. (ii-α) Averaged concentration vs. time responses taken at oxidation potential α in control (blue) and 1 h after intra-peritoneal SKF 91488 (50 mg/kg) administration (black) (n = 5 ± SEM). (ii-β) Averaged concentration vs. time responses taken at oxidation potential β in control (blue) and 1 h after intra-peritoneal SKF 91488 (50 mg/kg) administration (black) (n = 5 ± SEM). The blue bars represent the durations of the stimulus (350 μA, 60 Hz and 120 pulses) and error bars are SEM. (iii) Averaged maximal 5-HT release concentration in control rats (a) and rats pre-treated with thioperamide (10 mg/kg) (b). The bars are averages of the maximal 5-HT release in control stimulations (blue) and after SKF 91488 (50 mg/kg) administration (n = 6 ± SEM).

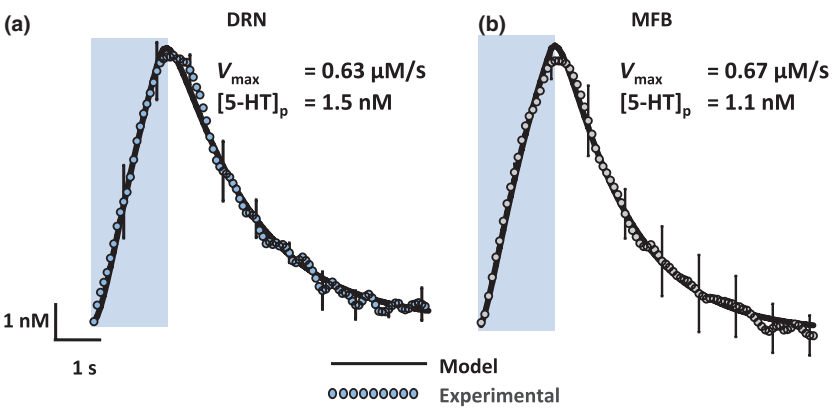

Fig. 6 A comparison of 5-HT experimental data and kinetic analysis between DRN and MFB stimulation. Averaged, normalized experimental data evoked by a 350 μA, 60 Hz and 120 pulse stimulation of the DRN (a) and the MFB (b) (blue dots, n = 6 ± SEM). Kinetically modeled data (black line) is superimposed and kinetic parameters V_{max} and $[5\text{-HT}]_p$ are inset when K_m is fixed at 170 nM. Blue box indicates duration of stimulation and error bars are SEM.

location and complicated topography of the DRN (Whishaw *et al.* 1977; Dib 1994). However, before this work, it had not been established whether electrical stimulation of the MFB at a location anterior to the terminal site (SNR) would release 5-HT. We had previously reported a similar phenomenon: the release of an unidentified substance in the red nucleus terminals upon anterior stimulation of the MFB (Kita *et al.* 2009). We suspected this substance was 5-HT, but since we had not yet optimized our electrochemical detection method with Nafion, we were unable to electrochemically verify this.

Because of our recent technological advances for *in vivo* 5-HT detection (Hashemi *et al.* 2009), we are able to study whether this phenomenon applies to 5-HT release in the SNR with MFB stimulation.

In Fig. 2, we compare the terminal output in the SNR upon DRN and MFB stimulation. Comparison of the inset cyclic voltammograms electrochemically confirms that 5-HT is released upon MFB stimulation. However, another substrate is present in the MFB cyclic voltammogram in Fig. 2(b). The main reductive process of 5-HT is delayed with both DRN and MFB stimulation and indeed in *in vitro* (inset β). However, the reduction associated with the other substrate occurs simultaneously with the oxidation (inset α) showing this substrate is electrochemically independent from 5-HT. While the second substrate overlaps with the voltammograms for 5-HT, it does not interfere with the concentration of 5-HT obtained at 0.65 V because its electrolysis peaks occur later in the cyclic voltammogram. We have previously found somatodendritic dopamine release in the ventral tegmental area upon MFB stimulation (Kita *et al.* 2009), however, because of the low levels of dopamine in the SNR (Heeringa and Abercrombie 1995) and the low sensitivity of the 5-HT specific waveform to dopamine (Hashemi *et al.* 2009), it is unlikely that there is a significant contribution from dopamine to this signal. Moreover, we had previously shown that the signal in the SNR is unresponsive to pharmacological manipulations by a dopamine transporter inhibitor, GBR 12909, when we stimulate the DRN (Hashemi *et al.* 2009). We also confirmed this to be true for MFB stimulation (data not shown).

Histamine is simultaneously released with 5-HT in the SNR during MFB stimulation

The oxidation and reduction peaks of the additional substrate occur on the backward sweep of the oxidation scan and the forward sweep of the reduction scan. Such features have been previously seen in fast-scan cyclic voltammetry (Pihel *et al.* 1995), and they are indicative of an electrochemical process that requires electrochemical cleaning of the electrode prior to its oxidation. Possible candidates based on these electrochemical characteristics are histamine, adenosine, or hydrogen peroxide (Pihel *et al.* 1998; Cechova and Venton 2008; Sanford *et al.* 2010). All three of these compounds are oxidized at very positive potentials and could be released by electrical stimulation of the medial forebrain bundle. We have previously shown that 5-HT itself can have distorted peaks when the electrode surface is fouled, but Nafion electrodeposition employed in our technique minimized this effect (Hashemi *et al.* 2009). Additionally, some groups have found 'switching' artifacts that occur at the switching potential of the waveform (Bull *et al.* 1990). The small current obtained at 0.85 V in Fig. 2(a-ii) may have contributions by such a switching artifact at around 1 V, however, the equivalent MFB stimulation causes a much larger current at 0.85 V (Fig. 2b-ii).

Collectively, the evidence presented in this paper indicates that histamine is the substance detected along with 5-HT. Histaminergic projections originate from the tuberomammillary nucleus (TM), located immediately ventral to the MFB, and traverse the MFB (Garbarg *et al.* 1974, 1976; Kohler *et al.* 1985; Panula *et al.* 1989). One of the target regions is the SNR where dense populations of histamine containing nerve terminals and histaminergic receptors are found (Panula *et al.* 1989; Schwartz *et al.* 1991). High amounts of histamine and histidine decarboxylase, the enzyme responsible for histamine synthesis from histidine, have been chemically verified in the SNR using microenzymatic methods (Pollard *et al.* 1978). Furthermore, the H-3 receptors present in the SNR (Cumming *et al.* 1991; Pollard *et al.* 1993; Anichtchik *et al.* 2000) have been shown to modulate GABA and 5-HT dynamics (Garcia *et al.* 1997; Korotkova *et al.* 2002; Threlfell *et al.* 2004). Thus, histamine release in the SNR following MFB stimulation is an anticipated result. Given the close locality of these two locations (MFB and TM), it is not possible to selectively stimulate the TM without activating the MFB. Thus, to gain more insight into the nature of the stimulation, we recorded maximal 5-HT and histamine release in the SNR while we lowered the stimulating electrode down the dorsal/ventral tract above our MFB coordinates in 0.5-mm intervals from 5.5 mm to 10 mm. Figure 2(c) shows that the maximal response for both 5-HT and histamine are at D/V 8.5 mm ($n = 6 \pm$ SEM) which is not surprising since this is the dorsal/ventral location of the MFB. However, the histamine response significantly peaks earlier than the 5-HT response dorsal to this location. This implies that the histaminergic fibers have a broader and independent fiber distribution through the MFB than the 5-HT fibers. In contrast to the MFB, the DRN has very little histaminergic innervation (Panula *et al.* 1989), explaining why stimulation of this region causes 5-HT release in the SNR with little or no histamine release.

Further evidence that the additional species is histamine comes from our electrochemical and pharmacological experiments. First, as shown in Fig. 3, the cyclic voltammetry of the unknown species closely resembles that for histamine in pH 7.4 solution. Second, administration of the highly selective ligand, SKF 91488, which potently inhibits histamine *N*-methyltransferase (Beaven and Shaff 1979), significantly increased the clearance time of the signal in comparison to the control with no effect on the signal amplitude [Panel (ii-α) of Fig. 5]. This drug also caused a significant decrease in the release amplitude of 5-HT after drug administration (β). Prior work has shown that activation of H-3 receptors inhibits 5-HT release (Threlfell *et al.* 2004). Since SKF 91488 prolongs histamine's life-time in the extracellular space, this would result in increased activation of H-3 receptors and suppression of 5-HT release. We confirm this by pre-treating rats with thioperamide (10 mg/kg), a highly selective H-3 receptor antagonist (Arrang *et al.*

1987) prior to SKF 91488 administration. Panel (iii) of Fig. 5 shows that thioperamide pre-treatment significantly arrests the SKF 91488 mediated inhibition of 5-HT release ($n = 6 \pm$ SEM).

Thus, on the basis of electrochemical, anatomical, physiological, and pharmacological evidence, we assign the second signal simultaneously released upon MFB stimulation to histamine.

The dynamic rate of electrically stimulated 5-HT release is independent of DRN or MFB stimulation

To confirm that MFB and DRN stimulations evoke release from a similar population of terminals in the SNR, we compared 5-HT signals obtained with each stimulation and compared kinetic parameters based on a model previously used to characterize 5-HT release in brain slices containing the SNR (Bunin and Wightman 1998). Figure 6 illustrates that there are no significant differences in $[5\text{-HT}]_p$ or V_{max} in the SNR with stimulation of the DRN or MFB. Furthermore, the calculated values of V_{max} in the SNR with both types of stimulation (0.63 and 0.67 μM/s, respectively) agree with ones previously established in tissue slice preparations (0.57 μM/s) (Bunin *et al.* 1998). Since V_{max} is a function of the number of active transporters, this term is expected to be the same in slices and *in vivo*. Thus, our finding of similar maximal uptake rates for 5-HT is consistent with removal of 5-HT by a transporter in each preparation.

However, these quantitative modeling studies reveal that 5-HT release evoked *in vivo* is much smaller than evoked in tissue slice preparations ($[5\text{-HT}]_p = 55$ nM in slices containing the SNR (Bunin *et al.* 1998) but 1.5 nM *in vivo* with MFB stimulation). This large difference in release amplitude may have contributed to the previous physical and analytical challenges of *in vivo* 5-HT voltammetric detection. It would appear that the local stimulations that were employed in the tissue slice preparation, bypassed the regulatory mechanisms that tightly control 5-HT release *in vivo*. This suggests that intact *in vivo* physiological mechanisms, combining both cell body and terminal feedback, may profoundly regulate 5-HT release. This regulation may be at the level of 5-HT autoreceptors (Blier *et al.* 1998; Daws *et al.* 2000), release of different vesicular pools (Pellegrino de Iraldi 1992), or activation of other inhibitory mechanisms (Invernizzi *et al.* 2007). These regulatory mechanisms, in combination with the fact that there is no known transporter for histamine, may also explain why the magnitude of histamine release is far greater than 5-HT release. These mechanisms are the focus of our ongoing studies.

In conclusion, this work shows that 5-HT release can be evoked by stimulating a collateral 5-HT projection in the MFB that branches to both the SNR and the striatum. We verified electrochemically, anatomically, physiologically and chemically that the additional species present upon MFB is histamine. We confirmed that MFB stimulation evokes 5-HT release that is quantitatively equivalent to that evoked by DRN stimulation; however, in both models, release is profoundly less than in tissue slice culture experiments. This highlights the importance of *in vivo* methods in exploring the mechanisms of 5-HT.

Acknowledgements

The authors thank Jessica Briley, Julie Gras-Najjar and Rinchen Lama for their experimental assistance. Department of Chemistry Electronics Facility designed and fabricated the instrumentation for these experiments. This research was supported by NIH (Grant NS15841 to R.M.W.).

References

Anichtchik O. V., Huotari M., Peitsaro N., Haycock J. W., Mannisto P. T. and Panula P. (2000) Modulation of histamine H3 receptors in the brain of 6-hydroxydopamine-lesioned rats. *Eur. J. Neurosci.* **12**, 3823–3832.

Arrang J. M., Garbarg M., Lancelot J. C., Lecomte J. M., Pollard H., Robba M., Schunack W. and Schwartz J. C. (1987) Highly potent and selective ligands for histamine H3-receptors. *Nature* **327**, 117–123.

Azmitia E. C. and Segal M. (1978) Autoradiographic analysis of differential ascending projections of dorsal and median raphe nuclei in rat. *J. Comp. Neurol.* **179**, 641–667.

Barnes N. M. and Sharp T. (1999) A review of central 5-HT receptors and their function. *Neuropharmacology* **38**, 1083–1152.

Beaven M. A. and Shaff R. E. (1979) New inhibitors of histamine-N-methyltransferase. *Biochem. Pharmacol.* **28**, 183–188.

Blier P., Pineyro G., el Mansari M., Bergeron R. and de Montigny C. (1998) Role of somatodendritic 5-HT autoreceptors in modulating 5-HT neurotransmission. *Ann. N Y Acad. Sci.* **861**, 204–216.

Borue X., Cooper S., Hirsh J., Condron B. and Venton B. J. (2009) Quantitative evaluation of serotonin release and clearance in Drosophila. *J. Neurosci. Methods* **179**, 300–308.

Borue X., Condron B. and Venton B. J. (2010) Both synthesis and reuptake are critical for replenishing the releasable serotonin pool in Drosophila. *J. Neurochem.* **113**, 188–199.

Brown R. E., Stevens D. R. and Haas H. L. (2001) The physiology of brain histamine. *Prog. Neurobiol.* **63**, 637–672.

Bull D. R., Palij P., Sheehan M. J., Millar J., Stamford J. A., Kruk Z. L. and Humphrey P. P. (1990) Application of fast cyclic voltammetry to measurement of electrically evoked dopamine overflow from brain slices in vitro. *J. Neurosci. Methods* **32**, 37–44.

Bunin M. A. and Wightman R. M. (1998) Quantitative evaluation of 5-hydroxytryptamine (serotonin) neuronal release and uptake: an investigation of extrasynaptic transmission. *J. Neurosci.* **18**, 4854–4860.

Bunin M. A., Prioleau C., Mailman R. B. and Wightman R. M. (1998) Release and uptake rates of 5-hydroxytryptamine in the dorsal raphe and substantia nigra reticulata of the rat brain. *J. Neurochem.* **70**, 1077–1087.

Cechova S. and Venton B. J. (2008) Transient adenosine efflux in the rat caudate-putamen. *J. Neurochem.* **105**, 1253–1263.

Corvaja N., Doucet G. and Bolam J. P. (1993) Ultrastructure and synaptic targets of the raphe-nigral projection in the rat. *Neuroscience* **55**, 417–427.

Cumming P., Shaw C. and Vincent S. R. (1991) High affinity histamine binding site is the H3 receptor: characterization and autoradio-

graphic localization in rat brain. *Synapse (New York, NY)* **8**, 144–151.

Davidson C. and Stamford J. A. (1996) Serotonin efflux in the rat ventral lateral geniculate nucleus assessed by fast cyclic voltammetry is modulated by 5-HT1B and 5-HT1D autoreceptors. *Neuropharmacology* **35**:1627–1634.

Daws L. C., Gould G. G., Teicher S. D., Gerhardt G. A. and Frazer A. (2000) 5-HT(1B) receptor-mediated regulation of serotonin clearance in rat hippocampus in vivo. *J. Neurochem.* **75**, 2113–2122.

Dib B. (1994) New technique for cannulae implantation into the dorsal raphe nucleus using layer 5 of cerebellum reference in rat stereotaxic surgery. *Pharmacol. Biochem. Behav.* **49**, 639–642.

Dray A., Gonye T. J., Oakley N. R. and Tanner T. (1976) Evidence for the existence of a raphe projection to the substantia nigra in rat. *Brain Res.* **113**, 45–57.

Fibiger H. C. and Miller J. J. (1977) Anatomical and electrophysiological investigation of serotonergic projection from dorsal raphe nucleus to substantia nigra in rat. *Neuroscience* **2**, 975–987.

Garbarg M., Barbin G., Feger J. and Schwartz J. C. (1974) Histaminergic pathway in rat brain evidenced by lesions of the medial forebrain bundle. *Science* **186**, 833–835.

Garbarg M., Barbin G., Bischoff S., Pollard H. and Schwartz J. C. (1976) Dual localization of histamine in an ascending neuronal pathway and in non-neuronal cells evidenced by lesions in the lateral hypothalamic area. *Brain Res.* **106**, 333–348.

Garcia M., Floran B., Arias-Montano J. A., Young J. M. and Aceves J. (1997) Histamine H3 receptor activation selectively inhibits dopamine D1 receptor-dependent [3H]GABA release from depolarization-stimulated slices of rat substantia nigra pars reticulata. *Neuroscience* **80**, 241–249.

Garris P. A. and Wightman R. M. (1994) Different kinetics govern dopaminergic transmission in the amygdala, prefrontal cortex, and striatum: an in vivo voltammetric study. *J. Neurosci.* **14**, 442–450.

Hafizi S., Kruk Z. L. and Stamford J. A. (1990) Fast cyclic voltammetry: improved sensitivity to dopamine with extended oxidation scan limits. *J. Neurosci. Methods* **33**, 41–49.

Hashemi P., Dankoski E. C., Petrovic J., Keithley R. B. and Wightman R. M. (2009) Voltammetric detection of 5-hydroxytryptamine release in the rat brain. *Anal. Chem.* **81**, 9462–9471.

Heeringa M. J. and Abercrombie E. D. (1995) Biochemistry of somatodendritic dopamine release in substantia nigra: an in vivo comparison with striatal dopamine release. *J. Neurochem.* **65**, 192–200.

Heien M. L., Phillips P. E., Stuber G. D., Seipel A. T. and Wightman R. M. (2003) Overoxidation of carbon-fiber microelectrodes enhances dopamine adsorption and increases sensitivity. *Analyst* **128**, 1413–1419.

Imai H., Steindler D. A. and Kitai S. T. (1986) The organization of divergent axonal projections from the midbrain raphe nuclei in the rat. *J. Comp. Neurol.* **243**, 363–380.

Invernizzi R. W., Pierucci M., Calcagno E., Di Giovanni G., Di Matteo V., Benigno A. and Esposito E. (2007) Selective activation of 5-HT(2C) receptors stimulates GABA-ergic function in the rat substantia nigra pars reticulata: a combined in vivo electrophysiological and neurochemical study. *Neuroscience* **144**, 1523–1535.

Jackson B. P., Dietz S. M. and Wightman R. M. (1995) Fast-scan cyclic voltammetry of 5-hydroxytryptamine. *Anal. Chem.* **67**, 1115–1120.

John C. E. and Jones S. R. (2007) Voltammetric characterization of the effect of monoamine uptake inhibitors and releasers on dopamine and serotonin uptake in mouse caudate-putamen and substantia nigra slices. *Neuropharmacology* **52**, 1596–1605.

John C. E., Budygin E. A., Mateo Y. and Jones S. R. (2006) Neurochemical characterization of the release and uptake of dopamine in ventral tegmental area and serotonin in substantia nigra of the mouse. *J. Neurochem.* **96**, 267–282.

Kita J. M., Kile B. M., Parker L. E. and Wightman R. M. (2009) In vivo measurement of somatodendritic release of dopamine in the ventral tegmental area. *Synapse* **63**, 951–960.

Kohler C., Swanson L. W., Haglund L. and Wu J. Y. (1985) The cytoarchitecture, histochemistry and projections of the tuberomammillary nucleus in the rat. *Neuroscience* **16**, 85–110.

van der Kooy D. and Hattori T. (1980) Dorsal raphe cells with collateral projections to the caudate-putamen and substantia nigra: a fluorescent retrograde double labeling study in the rat. *Brain Res.* **186**, 1–7.

Korotkova T. M., Haas H. L. and Brown R. E. (2002) Histamine excites GABAergic cells in the rat substantia nigra and ventral tegmental area in vitro. *Neurosci. Lett.* **320**, 133–136.

Kristensen E. W., Wilson R. L. and Wightman R. M. (1986) Dispersion in flow-injection analysis measured with microvoltammetric electrodes. *Anal. Chem.* **58**, 986–988.

Kristensen E. W., Kuhr W. G. and Wightman R. M. (1987) Temporal characterization of perfluorinated ion exchange coated microvoltammeteric electrodes for in vivo use. *Anal. Chem.* **59**, 1752–1757.

Michael D., Travis E. R. and Wightman R. M. (1998) Color images for fast-scan CV measurements in biological systems. *Anal. Chem.* **70**, 586A–592A.

Miller J. J., Richardson T. L., Fibiger H. C. and McLennan H. (1975) Anatomical and electrophysiological identification of a projection from the mesencephalic raphe to the caudate-putamen in the rat. *Brain Res.* **97**, 133–136.

Moore R. Y., Halaris A. E. and Jones B. E. (1978) Serotonin neurons of the midbrain raphe: ascending projections. *J. Comp. Neurol.* **180**, 417–438.

Mosko S. S., Haubrich D. and Jacobs B. L. (1977) Serotonergic afferents to the dorsal raphe nucleus: evdience from HRP and synaptosomal uptake studies. *Brain Res.* **119**, 269–290.

O'Connor J. J. and Kruk Z. L. (1991) Fast cyclic voltammetry can be used to measure stimulated endogenous 5-hydroxytryptamine release in untreated rat brain slices. *J. Neurosci. Methods* **38**, 25–33.

Panula P., Pirvola U., Auvinen S. and Airaksinen M. S. (1989) Histamine-immunoreactive nerve fibers in the rat brain. *Neuroscience* **28**, 585–610.

Parent A., Descarries L. and Beaudet A. (1981) Organization of ascending serotonin systems in the adult rat brain. A radioautographic study after intraventricular administration of [3H]5-hydroxytryptamine. *Neuroscience* **6**, 115–138.

Park J., Kile B. M. and Wightman R. M. (2009) In vivo voltammetric monitoring of norepinephrine release in the rat ventral bed nucleus of the stria terminalis and anteroventral thalamic nucleus. *Eur. J. Neurosci.* **30**, 2121–2133.

Paxinos G. and Watson C. (2007) *The Rat Brain in Stereotaxic Coordinates*, 6th Edn. Elsevier, London, UK.

Pellegrino de Iraldi A. (1992) Compartmentalization of monoaminergic synaptic vesicles in the storage and release of neurotransmitter. *Mol. Neurobiol.* **6**, 323–337.

Petty F., Davis L. L., Kabel D. and Kramer G. L. (1996) Serotonin dysfunction disorders: a behavioral neurochemistry perspective. *J. Clin. Psychiatry* **57**(Suppl 8), 11–16.

Pihel K., Hsieh S., Jorgenson J. W. and Wightman R. M. (1995) Electrochemical detection of histamine and 5-hydroxytryptamine at isolated mast cells. *Anal. Chem.* **67**, 4514–4521.

Pihel K., Hsieh S., Jorgenson J. W. and Wightman R. M. (1998) Quantal corelease of histamine and 5-hydroxytryptamine from mast cells and the effects of prior incubation. *Biochemistry* **37**, 1046–1052.

Pollard H., Llorens-Cortes C., Barbin G., Garbarg M. and Schwartz J. C. (1978) Histamine and histidine decarboxylase in brain stem nuclei: distribution and decrease after lesions. *Brain Res.* **157**, 178–181.

Pollard H., Moreau J., Arrang J. M. and Schwartz J. C. (1993) A detailed autoradiographic mapping of histamine H3 receptors in rat brain areas. *Neuroscience* **52**, 169–189.

Rice M. E., Richards C. D., Nedergaard S., Hounsgaard J., Nicholson C. and Greenfield S. A. (1994) Direct monitoring of dopamine and 5-HT release in substantia nigra and ventral tegmental area in vitro. *Exp. Brain Res.* **100**, 395–406.

Robinson D. L. and Wightman R. M. (2007) Rapid dopamine release in freely moving rats, in *Electrochemical Methods for Neuroscience* (Michael A. C. and Borland L. M., eds), pp. 17–36. CRC Press, Boca Raton, FL.

Rueter L. E., Fornal C. A. and Jacobs B. L. (1997) A critical review of 5-HT brain microdialysis and behavior. *Rev. Neurosci.* **8**, 117–137.

Sanford A. L., Morton S. W., Whitehouse K. L., Oara H. M., Lugo-Morales L. Z., Roberts J. G. and Sombers L. A. (2010) Voltammetric detection of hydrogen peroxide at carbon fiber microelectrodes. *Anal. Chem.* **82**, 5205–5210.

Schwartz J. C., Arrang J. M., Garbarg M., Pollard H. and Ruat M. (1991) Histaminergic transmission in the mammalian brain. *Physiol. Rev.* **71**, 1–51.

Shaskan E. G. and Snyder S. H. (1970) Kinetics of serotonin accumulation into slices from rat brain: relationship to catecholamine uptake. *J. Pharmacol. Exp. Ther.* **175**, 404–418.

Steinbusch H. W., van der Kooy D., Verhofstad A. A. and Pellegrino A. (1980) Serotonergic and non-serotonergic projections from the nucleus raphe dorsalis to the caudate-putamen complex in the rat, studied by a combined immunofluorescence and fluorescent retrograde axonal labeling technique. *Neurosci. Lett.* **19**, 137–142.

Steinbusch H. W., Nieuwenhuys R., Verhofstad A. A. and Van der Kooy D. (1981) The nucleus raphe dorsalis of the rat and its projection upon the caudatoputamen. A combined cytoarchitectonic, immunohistochemical and retrograde transport study. *J. Physiol. (Paris)* **77**, 157–174.

Takmakov P., Zachek M. K., Keithley R. B., Walsh P. L., Donley C., McCarty G. S. and Wightman R. M. (2010) Carbon microelectrodes with a renewable surface. *Anal. Chem.* **82**, 2020–2028.

Threlfell S., Cragg S. J., Kallo I., Turi G. F., Coen C. W. and Greenfield S. A. (2004) Histamine H3 receptors inhibit serotonin release in substantia nigra pars reticulata. *J. Neurosci.* **24**, 8704–8710.

Threlfell S., Greenfield S. A. and Cragg S. J. (2010) 5-HT(1B) receptor regulation of serotonin (5-HT) release by endogenous 5-HT in the substantia nigra. *Neuroscience* **165**, 212–220.

Whishaw I. Q., Cioe J. D., Previsich N. and Kolb B. (1977) The variability of the interaural line vs the stability of bregma in rat stereotaxic surgery. *Physiol. Behav.* **19**, 719–722.

Wightman R. M., Amatore C., Engstrom R. C., Hale P. D., Kristensen E. W., Kuhr W. G. and May L. J. (1988) Real-time characterization of dopamine overflow and uptake in the rat striatum. *Neuroscience* **25**, 513–523.

Wirtshafter D., Stratford T. R. and Asin K. E. (1987) Evidence that serotonergic projections to the substantia nigra in the rat arise in the dorsal, but not the median, raphe nucleus. *Neurosci. Lett.* **77**, 261–266.